

Lattice dynamical implication of ilmenite MgXO_3 (X=Si, Ge, Ti) using Raman spectroscopy at high-pressures and high-temperatures

*T. Okada**, T. Narita, T. Nagai and T. Yamanaka

Dep. Earth and Space Science, Osaka Univ., Toyonaka, Osaka 560-0043, Japan

okataku@ess.sci.osaka-u.ac.jp

Abstract

High-temperature and high-pressure Raman spectra of ilmenite-type $\text{MgX}^{4+}\text{O}_3$ (X=Si, Ge, Ti) have been collected up to 773 K, and 31.3, 22.4 and 12.0 GPa, respectively. Temperature and pressure dependence of the force constant of X-O stretching bands revealed that mechanisms of expansion and compression of XO_6 octahedra are different in three ilmenites. The tendency is consistent with thermodynamic stability of three ilmenites. From the Raman frequency shifts with temperature and pressure, intrinsic anharmonic effects on isochoric specific heat were elucidated. The anharmonic effects are related to the Debye temperature of three ilmenites.

Introduction

Ilmenite-type MgSiO_3 is one of high-pressure polymorphs of enstatite, and characterized by a relatively narrow stability field in the 20-24 GPa and 1400-2300 K range (Sawamoto 1987). Since MgSiO_3 -ilmenite is stable at thermodynamically low temperature, it is considered to be a candidate component in 600-700 km of subducting slabs. $(\text{Mg,Fe})\text{SiO}_3$ -ilmenite was found in the shock vein of meteorite and named akimotoite (Tomioka and Fujino 1997). It is important for earth science to understand the stability of its crystal structure at high pressure and temperature. The crystal structure of MgSiO_3 ilmenite was analysed by single crystal X-ray diffraction study under ambient conditions (Horiuchi et al. 1982) and by Rietveld profile fitting at high pressure (Reynard et al. 1996). Molecular dynamics simulations of MgSiO_3 ilmenite have been also carried out (Matsui et al. 1987; Karki et al. 2000). ABO_3 -ilmenite structure has unique face-shared and edge-shared configurations of AO_6 and BO_6 octahedra. Cation-cation interactions in the structure have a significant meaning for the degree of disorder and physical properties.

Raman spectroscopic studies provide the information about vibration of each atom and thus a crystal structure can be discussed on the basis of lattice dynamics such as interatomic strength and bonding energy. The spectroscopy is a complementary method to X-ray diffraction study that analyses the static crystal structure. High-pressure and high-temperature Raman spectra of ilmenite-type MgSiO_3 have already been investigated up to 7 GPa and 1030 K, respectively (Reynard and Rubie 1996). In this study, from the viewpoint that the bond strength influences the interatomic distances, we obtained Raman spectra under thermodynamic stable condition of ilmenite and clarified the mechanism of the thermal expansion and pressurized compression of ilmenite structure.

$\text{MgX}^{4+}\text{O}_3$ (X=Si, Ge, Ti) ilmenites have various stable P-T regions due to their compositions, i.e., the cation radius ratios: MgSiO_3 -, MgGeO_3 - and MgTiO_3 -ilmenite is stable at high-pressures, moderate-pressures and ambient pressure, respectively (Ross and Navrotsky 1988; Linton et al. 1999). Yamanaka et al. (2005, in press) has conducted single-crystal diffraction study under high pressures on ilmenites of MgSiO_3 , MgGeO_3 and MgTiO_3 and obtained interatomic distances, bond angles and bulk moduli of their unit cell and octahedral volumes. In this study, we conducted a high-pressure, high-temperature Raman spectroscopic study of MgSiO_3 , MgGeO_3 and MgTiO_3 ilmenites. We investigate the elastic properties and bonding characters of ilmenite at high pressure and high temperature and discuss the compositional dependence of their structure changes.

Anharmonic contribution to the thermodynamic properties of mantle minerals is one of the significant problems of geophysics. In the previous vibrational models of the high-pressure phases, it was commonly assumed that the quasi-harmonic approximation, hence the Dulong and Petit limit for the isochoric specific heat at high temperature. However, in fact, this approximation fails at high temperature because of intrinsic anharmonic effects. Since the Raman spectra recorded at various high temperatures and pressures reveal the Grüneisen parameters and the intrinsic anharmonic mode parameter, we present here the results obtained and discuss the anharmonic effects on the thermodynamic properties such as the isochoric specific heat.

Experimental Method

Powdered sample of MgSiO₃-enstatite was synthesized at ambient pressure and 1800 K for 40 h by solid-solid reaction of MgO and SiO₂ using MoSi₂ electric furnace under atmospheric condition. It was used as a starting material and transformed at 22 GPa and 1800 K for 30 min using 5000 ton multi-anvil press installed at Misasa, Okayama University. A semi-sintered MgO octahedron was used as the pressure medium and a cylindrical Re foil was used as the sample chamber and as the furnace in conjunction with a Ta electrode. The furnace was surrounded by LaCrO₃ as a thermal insulator. MgGeO₃-ilmenite was synthesized at 6 GPa and 1200 K for 17 h using cubic-anvil press installed at Osaka University. A pyrophyllite cube was used as the pressure medium and a graphite sleeve as the heating material. The starting material of mixture of MgO and GeO₂ was kept in gold tubes sealed at both ends by welding to refrain samples from reducing. MgTiO₃-ilmenite was prepared by solid-solid reaction of MgO and TiO₂ in Pt crucible at ambient pressure and 1800 K for 80 h using MoSi₂ electric furnace under atmospheric condition. To obtain the homogeneous sample, the recovered sample was pulverized and sintered again on the same conditions. The purity and homogeneity of the three samples were confirmed by both microprobe chemical analyses and X-ray powder diffractions.

Raman spectra were obtained using the NRS2100-F laser Raman spectrometer (JASCO, Japan) equipped with a triple-grating monochromator and an Ar ion laser at 514.5 nm. The incident laser beam was focused on the sample using an 20X objective lens (working distance 21.0 mm, SLMPlan, Olympus, Japan). Raman shifts were calibrated with Ne lamp spectrum as the standard. High-temperature experiments were performed using a heating stage consisted of a Pt-electric resistance heater with a water-cooled system and a Pyrex glass window. Temperature was monitored with a chromel-almel thermocouple. High-temperature Raman spectra of each sample were collected up to 773 K at ambient pressure for 300 s exposure time per point with the operating laser power of 200mW (for MgSiO₃), for 30 s with 70 mW (for MgGeO₃) and for 5 s with 80 mW (for MgTiO₃), respectively. For high-pressure experiments, a diamond-anvil cell (DAC) was used. The diameter of culet of diamond is 350 μm. A spring steel gasket with 200 μm in thickness was preindented to 50 μm and a sample cavity of 130 μm in diameter was opened using an electric discharge machining. The powdered sample was loaded with H₂O as pressure medium and small ruby chips (10 μm in diameter) for pressure measurements. H₂O was preferred to an alcohol mixture as the pressure medium because it has no strong Raman bands in the measured region. Pressures were determined from the shift of the ruby fluorescence R1 line (Mao et al. 1978), excited by the Ar ion laser. High-pressure Raman spectra of each sample were collected at room temperature and up to 31.3 GPa for 300 s exposure time per point with the operating laser power of 600mW (for MgSiO₃), up to 22.4 GPa for 100 s with 250 mW (for MgGeO₃) and up to 12.0 GPa for 100 s with 150 mW (for MgTiO₃), respectively. We decided the center of each peak by fitting using a Gaussian function with optimising variables of peak position, peak height and half width (FWHM).

Results and Discussion

Temperature and pressure dependence of Raman spectra

For the ilmenite structure, factor group analysis (e.g., Fateley et al. 1971; Ross and McMillan 1984) gives the number and symmetries of expected bands:

$$\Gamma = 5A_g(\text{Raman}) + 5E_g(\text{Raman}) + 4A_u(\text{IR}) + 4E_u(\text{IR}). \quad (1)$$

Hofmeister (1993) compared the reported previous Raman spectra of eight different ilmenite compounds (MgSiO_3 , ZnSiO_3 , MgGeO_3 , ZnGeO_3 , MgTiO_3 , MnTiO_3 , ZnTiO_3 and CdTiO_3) and assigned ten Raman active modes (Table 1): $A_g(1)$ and $E_g(1)$ were assigned to X^{4+} -O stretching bands, $A_g(4)$ and $E_g(4)$ to translations of the XO_6 octahedra against M^{2+} , $A_g(5)$ and $E_g(5)$ to translations of the M^{2+} cation against the oxygen framework, and the remaining bands to bends of O-X^{4+} -O. Under ambient conditions, we could observe seven (for MgSiO_3), eight (for MgGeO_3) and ten (for MgTiO_3) Raman bands, respectively (Table 1). For MgSiO_3 - and MgGeO_3 -ilmenite, some Raman peaks could not be observed. The frequencies of Raman bands from each ilmenite under ambient conditions are in agreement with previous determinations (McMillan and Ross 1987 (for MgSiO_3); Ross and Navrotsky 1987 (for MgGeO_3); White 1974 (for MgTiO_3)).

Table 1 Vibrational mode assignment, frequencies under ambient conditions, temperature and pressure derivatives of the frequencies of ilmenite-type MgSiO_3 , MgGeO_3 and MgTiO_3 .

Symmetry	Assignment	ν_i [cm^{-1}]			$-(\delta\nu_i/\delta T)_p$ [$\text{cm}^{-1}\text{K}^{-1}$]			$(\delta\nu_i/\delta P)_T$ [$\text{cm}^{-1}\text{K}^{-1}$]		
		MgSiO_3	MgGeO_3	MgTiO_3	MgSiO_3	MgGeO_3	MgTiO_3	MgSiO_3	MgGeO_3	MgTiO_3
$A_g(1)$	X-O stretch	802	719	714	0.016	0.021	0.010	3.825	3.909	3.580
$A_g(2)$	X-O-X bend	622	474	487	0.018	0.026	0.026	3.268	3.300	3.294
$A_g(3)$	X-O-X bend	481	377	352	0.028	0.017	0.021	2.822	2.213	2.863
$A_g(4)$	$T(\text{XO}_6)$	412	330	327	0.021	0.011	0.010	2.068	1.208	2.233
$A_g(5)$	T(Mg)	352		281	0.012		0.017			1.558
$E_g(1)$	X-O stretch	687	615	641	0.016	0.021	0.011	3.413	3.370	4.689
$E_g(2)$	X-O-X bend		451	485		0.011			2.909	
$E_g(3)$	X-O-X bend			397			0.011			2.813
$E_g(4)$	$T(\text{XO}_6)$		314	306		0.015	0.017		2.028	2.006
$E_g(5)$	T(Mg)	291	202	224	0.013	0.016	0.023		1.080	1.587

For high-temperature experiments, Raman spectrum of each ilmenite was obtained at temperatures of 293 K, 373 K, 473 K, 573 K, 673 K and 773 K, which is maximum temperature for the heating stage. We observed no softmode and no transformation of each ilmenite up to 773 K. With increasing temperature, each band shifted to lower frequency (Fig. 1a-c). The Raman frequency shifts with temperature obtained from a linear regression of the high-temperature data are reported in Table 1 and Fig. 3a. During decreasing temperature, no hysteresis was observed.

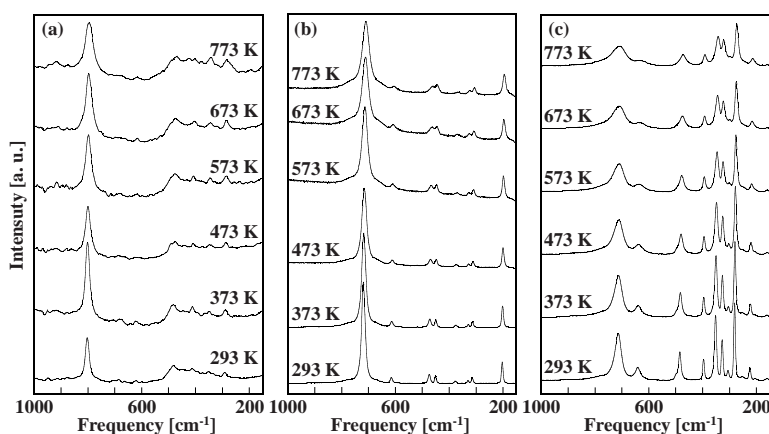


Fig. 1 Temperature dependence of the Raman spectra of ilmenite-type (a) MgSiO_3 , (b) MgGeO_3 and (c) MgTiO_3 .

For high-pressure experiments, Raman spectrum of each ilmenite was obtained up to the pressure considered to be the thermodynamically stable region of each ilmenite at room temperature. We observed no softmode and no transformation of each ilmenite during

compression. With increasing pressure, each band shifted to higher frequency (Fig. 2a-c). The Raman frequency shifts with pressure obtained from a linear regression of the high-pressure data are also reported in Table 1 and Fig. 3b. For MgSiO₃ and MgGeO₃, some bands could not be observed at high-pressure, because the overall intensity of the Raman spectrum was decreased dramatically with pressure. During decompression, no hysteresis was observed.

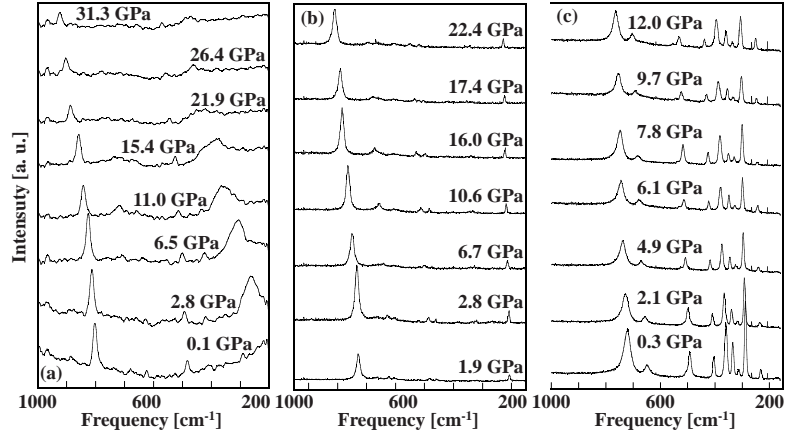


Fig. 2 Pressure dependence of the Raman spectra of ilmenite-type (a) MgSiO₃, (b) MgGeO₃ and (c) MgTiO₃.

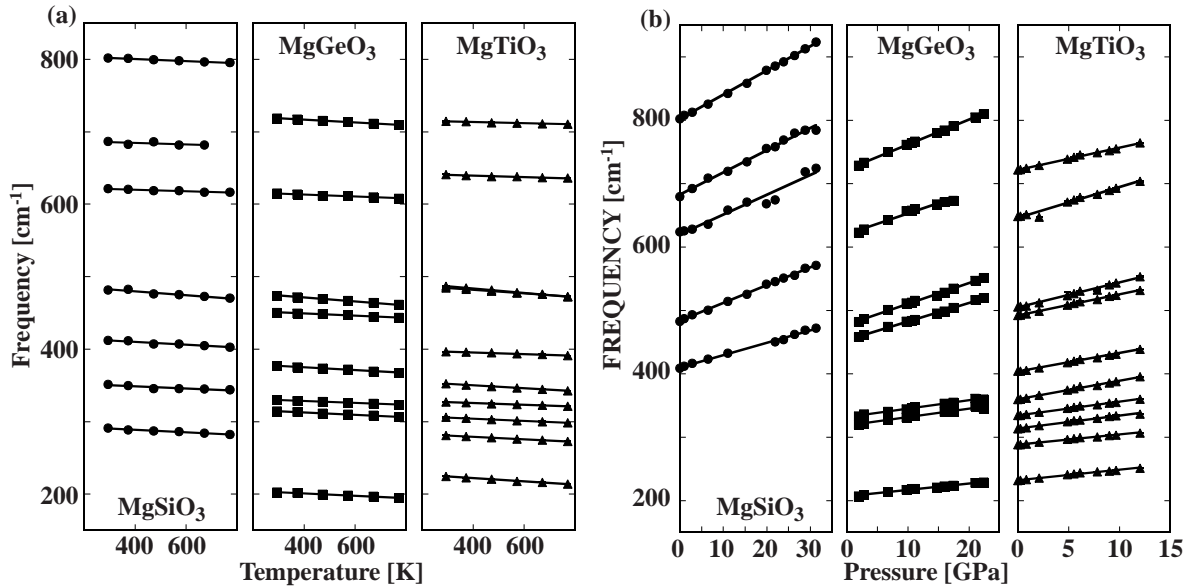


Fig. 3 Evolution of Raman frequencies of ilmenite-type MgSiO₃, MgGeO₃ and MgTiO₃ with (a) temperature and (b) pressure.

Temperature and pressure dependence of the force constant, k

In order to discuss the lattice dynamics, the force constant, k , expressing the bond strength between atoms is used. The force constant, k , could be expressed approximately by the following equation:

$$\nu = \frac{1}{2c} \sqrt{\frac{k}{\mu}} \quad \text{or} \quad k = 4c^2 \mu \nu^2 \quad (2)$$

where ν is the stretching vibrational frequency of the stretching band. The reduced mass μ of the two-mass system is expressed as follow:

$$\frac{1}{\mu} = \frac{1}{m_1} + \frac{1}{m_2} \quad \text{or} \quad \mu = \frac{m_1 m_2}{m_1 + m_2} \quad (3)$$

where m_1 and m_2 are the atomic weights of both ends. In this study, there are two X-O stretching bands (A_g(1) and E_g(1)) for each ilmenite. We calculated k from the bands at each condition, and obtained the pressure and temperature derivatives of k (Fig.4 and Table 2). For XO₆ octahedra of ilmenite structure, there are two types of X-O bonds: a longer X-O opposed

to the shared face in MgO₆ octahedron and a shorter X-O bond opposed to the unshared face. In general, a shorter bond has stronger bond strength. A_g(1) mode is higher frequency and has a larger k -value than E_g(1) mode. Hence it is considered to be a stronger bond, that is, a shorter X-O bond facing to the unshared face in MgO₆, and vice versa.

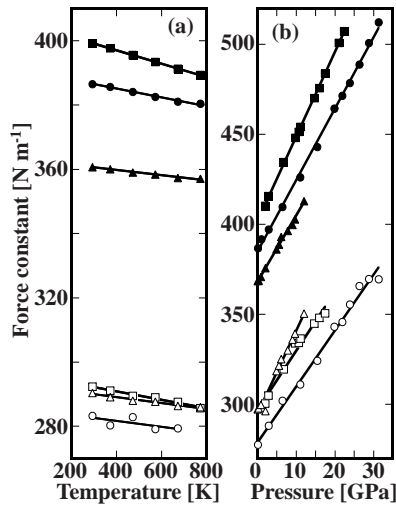


Fig. 4 Evolution of the force constant, k , with (a) temperature and (b) pressure. Solid circles represent A_g(1) of Si-O stretching band; open circle, E_g(1) of Si-O; solid squares, A_g(1) of Ge-O; open squares, E_g(1) of Ge-O; solid triangles, A_g(1) of Ti-O; open triangles, E_g(1) of Ti-O.

Table 2 Temperature and pressure derivatives of k .

	$-(\delta k / \delta T)$ [$10^{-4} \text{Nm}^{-1} \text{GPa}^{-1}$]		$(\delta k / \delta P)$ [$10^{-2} \text{Nm}^{-1} \text{GPa}^{-1}$]	
	A _g (1)	E _g (1)	A _g (1)	E _g (1)
Si-O stretch	136(7)	92(50)	397(6)	310(10)
Ge-O stretch	209(2)	131(9)	468(3)	328(19)
Ti-O stretch	81(5)	90(9)	366(8)	460(24)

The temperature derivatives of k of both A_g(1) and E_g(1) were the order of Ge-O, Si-O and Ti-O stretching bands (Table 2). Generally, the large variation of k with temperature or pressure is attributed to the weakness of the bond strength. The tendency gives an effect on the relative expansion rate for each XO₆ octahedron: the expansion rate is the order of GeO₆, SiO₆ and TiO₆ octahedron. This is consistent with the fact that only MgTiO₃-ilmenite is a thermodynamically stable phase among three samples in the present high-temperature experimental region. MgGeO₃- and MgSiO₃-ilmenite are unstable in the region. Si-O bond is stronger than Ge-O bond: SiO₆ in MgSiO₃ may be more rigid octahedron than GeO₆, because MgSiO₃-ilmenite is stable at much higher pressure than MgGeO₃.

The pressure derivative of k of A_g(1) of Ge-O bond is more noticeable compared with those of Si-O and Ti-O bonds (Table 2). This is consistent with the fact that the order of the bulk modulus of XO₆ octahedra (Yamanaka et al. 2005, in press; Table 4; $K_{T, \text{SiO}_6} = 268(26)$ GPa, $K_{T, \text{GeO}_6} = 218(15)$ GPa and $K_{T, \text{TiO}_6} = 261(22)$ GPa). However, the order of the pressure derivatives of k of E_g(1) in three samples is quite different from those of the A_g(1) mode as seen in Table 2. For Si-O and Ge-O bonds, the pressure derivatives of k of A_g(1) are larger than those of E_g(1). Namely, shorter X-O bonds (A_g(1)) opposed to the unshared face in MgO₆ are more shortened under pressure than longer X-O bonds (E_g(1)) facing to the shared face, indicating that the distortion of XO₆ octahedra is enhanced at higher pressures. For Ti-O bond, the pressure derivative of k of A_g(1) is smaller than that of E_g(1). Namely, longer Ti-O bond (E_g(1)) is more shortened under pressure than shorter Ti-O bond (A_g(1)), indicating that the regularity of TiO₆ octahedra is enhanced at higher pressures. These phenomena are consistent with the pressure dependence of interatomic distances decided by the single-crystal X-ray structure analyses under high pressures (Yamanaka et al. 2005, in press; Fig.3).

Anharmonic effect on the thermodynamic properties

From the obtained frequency shifts with pressure and temperature, the isothermal and isobaric Grüneisen parameters, γ_{iT} and γ_{iP} , can be calculated as follows (Gillet et al. 1989),

$$\gamma_{iT} = - \left(\frac{\partial \ln \nu_i}{\partial \ln V} \right)_T = - \left(\frac{\partial V}{\partial \ln V} \right)_T \left(\frac{\partial P}{\partial V} \right)_T \left(\frac{\partial \ln \nu_i}{\partial P} \right)_T = -V \left(\frac{\partial P}{\partial V} \right)_T \left(\frac{\partial \ln \nu_i}{\partial P} \right)_T = K_T \left(\frac{\partial \ln \nu_i}{\partial P} \right)_T \quad (4)$$

$$\gamma_{iP} = - \left(\frac{\partial \ln \nu_i}{\partial \ln V} \right)_P = - \left(\frac{\partial V}{\partial \ln V} \right)_P \left(\frac{\partial T}{\partial V} \right)_P \left(\frac{\partial \ln \nu_i}{\partial T} \right)_P = -V \left(\frac{\partial T}{\partial V} \right)_P \left(\frac{\partial \ln \nu_i}{\partial T} \right)_P = - \frac{1}{\alpha} \left(\frac{\partial \ln \nu_i}{\partial T} \right)_P \quad (5)$$

where ν_i is the vibrational frequency of the i^{th} band, K_T is the isothermal bulk modulus, and α is the thermal expansivity. We used $\alpha=2.44 \times 10^{-5} \text{ K}^{-1}$ and $K_T=224 \text{ GPa}$ for MgSiO_3 , $\alpha=2.23 \times 10^{-5} \text{ K}^{-1}$ and $K_T=180 \text{ GPa}$ for MgGeO_3 , and $\alpha=3.00 \times 10^{-5} \text{ K}^{-1}$ and $K_T=158 \text{ GPa}$ for MgTiO_3 (Ashida et al. 1988, 1985; Wechsler and Prewitt 1984; Yamanaka et al. 2005, in press). The values of calculated γ_{iT} and γ_{iP} of each vibrational band are reported in Table 3. The intrinsic anharmonic mode parameter, a_i , can be also calculated using the values of the isothermal and isobaric Grüneisen parameters as follow (Gillet et al. 1989),

$$a_i = \left(\frac{\partial \ln \nu_i}{\partial T} \right)_V = \alpha K_T \left(\frac{\partial \ln \nu_i}{\partial P} \right)_T - \left(\frac{\partial \ln \nu_i}{\partial T} \right)_P = \alpha (\gamma_{iT} - \gamma_{iP}). \quad (6)$$

The values of calculated a_i of each vibrational band are reported in Table 3 and Fig. 5. Their absolute values are not significantly different from zero for the high-frequency bands but they become large while the frequency becomes low. Note that the absolute values of a_i for the internal modes of XO_6 octahedra (X-O stretching or X-O-X bending bands) are smaller than those for the lattice modes (translation bands of XO_6 or Mg cation).

Table 3 The values of calculated γ_{iP} , γ_{iT} and a_i of each vibrational band.

Symmetry	MgSiO_3				MgGeO_3				MgTiO_3			
	ν_i	γ_{iP}	γ_{iT}	$a_i [10^{-5} \text{K}^{-1}]$	ν_i	γ_{iP}	γ_{iT}	$a_i [10^{-5} \text{K}^{-1}]$	ν_i	γ_{iP}	γ_{iT}	$a_i [10^{-5} \text{K}^{-1}]$
$E_g(5)$	291	2.41(15)			202	3.67(2)	0.84(3)	-6.31(11)	234	3.38(8)	1.09(4)	-6.88(38)
$A_g(5)$	352	1.76(42)							281	2.06(2)	0.84(2)	-3.66(13)
$E_g(4)$					314	2.35(3)	0.71(4)	-3.66(15)	306	1.75(5)	0.99(4)	-2.28(26)
$A_g(4)$	412	2.00(19)	1.00(2)	-2.44(52)	330	1.77(3)	0.69(3)	-2.42(12)	327	1.19(1)	0.98(3)	-0.63(12)
$A_g(3)$	481	2.19(31)	1.20(2)	-2.41(80)	377	2.33(13)			352	1.97(3)	1.24(3)	-2.21(17)
$E_g(3)$									397	0.93(1)	1.09(2)	0.48(10)
$E_g(2)$					451	1.55(7)	1.09(2)	-1.03(19)	485	1.72(4)	1.03(2)	-2.07(18)
$A_g(2)$	622	0.69(9)	1.05(8)	0.86(40)	474	2.53(4)	1.15(3)	-3.08(15)	487	2.21(5)	1.18(3)	-3.10(25)
$E_g(1)$	687	0.67(37)	1.07(4)	0.97(99)	615	1.01(7)	0.91(6)	-0.24(29)	641	0.52(5)	1.14(6)	1.84(34)
$A_g(1)$	802	0.73(4)	1.00(1)	0.67(11)	719	1.18(1)	0.92(1)	-0.58(5)	714	0.38(2)	0.75(2)	1.11(12)
Average		1.16	1.06	-0.47		2.05	0.90	-2.47		1.61	1.03	-1.74

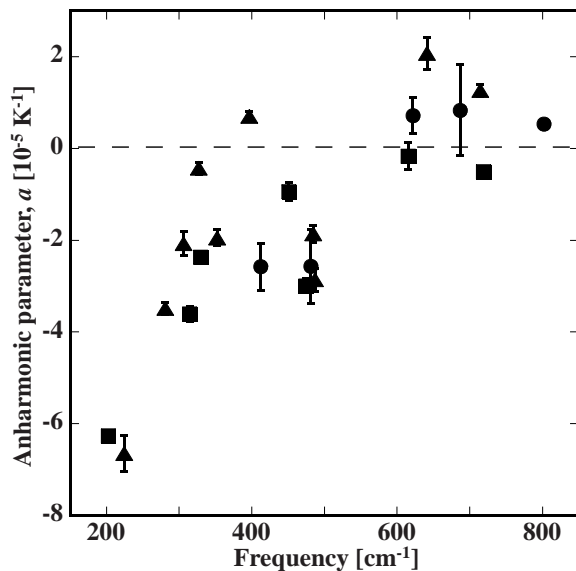


Fig. 5 Anharmonic parameters of each vibrational band. Solid circles represent MgSiO_3 ; solid squares, MgGeO_3 ; solid triangles, MgTiO_3 .

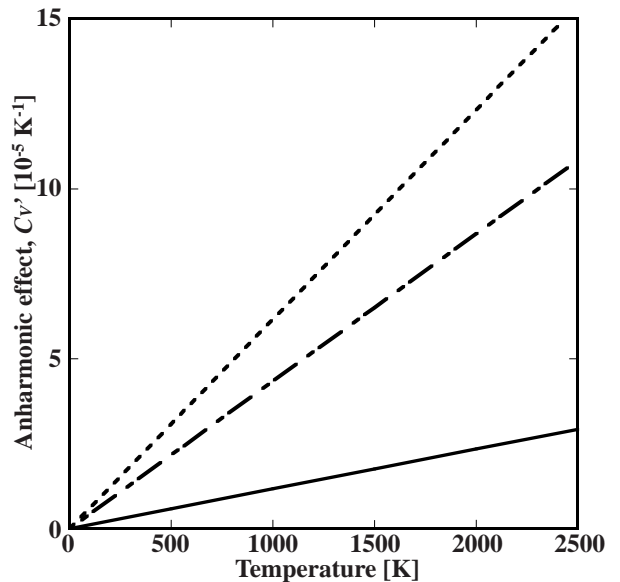


Fig. 6 Temperature dependence of the calculated anharmonic effect on the specific heat. Solid line represents MgSiO_3 ; dashed line, MgGeO_3 ; dot-dashed line, MgTiO_3 .

With the anharmonic contribution, the isochoric specific heat is expressed as follow (Gillet et al. 1991):

$$C_V = 3nR \sum_{i=1}^m C_{Vi}^h (1 - 2a_i T) \quad (7)$$

where n is the number of atoms in the mineral formula, R is the gas constant, C_{Vi}^h is the harmonic part of the isochoric specific heat of the i^{th} mode. To ensure the consistency with the calculation of the harmonic contribution to C_V and compare the difference of the anharmonic effect by chemical composition in the three ilmenites, the average intrinsic anharmonic mode parameter of a_i in each vibrational band, \bar{a} , was used (Table 3). The anharmonic effect on the specific heat, C_V' , can be approximated with $-6n\bar{a}RT$. Similarly, for the entropy S and relative enthalpy ΔH , it can be approximated with $-6n\bar{a}RT$ for S' and $-3n\bar{a}RT$ for $\Delta H'$, respectively (Reynard et al. 1996b). From the obtained \bar{a} , the C_V' was calculated for each ilmenite and showed the relation against temperature in Fig. 6. The C_V' was the order of MgGeO₃, MgTiO₃ and MgSiO₃. At 773 K, maximum temperature in this study, C_V' was estimated to be $<5 \text{ J mol}^{-1} \text{ K}^{-1}$ even for MgGeO₃. Thus, the intrinsic anharmonic corrections to the lattice dynamical discussion concerning the force constant are insignificant. However, as shown in Fig. 6, as it becomes higher temperature exceeding the Debye temperature, the anharmonic effects are larger. The Debye temperature, Θ_D , can be obtained approximately as follow (Poirier 1991),

$$\Theta_D = 251.2 \left(\frac{\rho}{\bar{M}} \right)^{\frac{1}{3}} v_m \quad (8)$$

where ρ is a density, \bar{M} is a mean atomic mass, and v_m is an average velocity of sound waves, v_P and v_S . The Debye temperatures, which were re-calculated from the reported values of ρ , v_P and v_S (Hofmeister and Ito 1992; Ashida et al. 1988, 1985; Weidner and Ito 1985; Liebermann 1976), are 1113 K for MgSiO₃, 819 K for MgGeO₃ and 849 K for MgTiO₃. The higher the Debye temperature is, the smaller the anharmonic effect on C_V at high temperature is. At high temperature as the Earth's deep mantle, it is expected that the actual anharmonic effect of MgSiO₃-ilmenite is much larger. In this study, we obtained the anharmonic effect of MgSiO₃-ilmenite from the Raman vibrational data up to 773 K and 31.3 GPa. The more precise anharmonic discussion requires the vibrational data obtained over the wider range of pressures and temperatures.

Conclusion

From the Raman spectra of ilmenite-type MgX⁴⁺O₃ (X=Si, Ge, Ti) at high temperatures and high pressures, temperature and pressure derivatives of the force constant of the X-O stretching bands were calculated. The mechanisms of expansion and compression of XO₆ octahedra are different in three ilmenites and consistent with the results of the single-crystal X-ray structure analyses as a function of pressure (Yamanaka et al. 2005, in press). The Raman vibrational frequency corresponds to the interatomic bond energy, which leads to the interatomic distance. Since high-pressure minerals are difficult to synthesize their single-crystals, the high-temperature and high-pressure Raman spectroscopic studies on the powdered samples are useful to clarify the mechanisms of expansion and compression, which give the light on the premonitory phenomena of transformation.

The present estimation of the anharmonic effect on the specific heat of MgSiO₃-ilmenite is very small. Generally, the interatomic potential well becomes deep under high pressure condition. The anharmonic effect is not so significant under thermodynamically low temperature condition. However, under such sufficiently high temperature condition as the Earth's deep mantle, the effect cannot be ignored. It is interesting to clarify the anharmonic effect of various mantle minerals using the method of the present study.

Acknowledgements

This study was supported by the Grant-in-Aid for the 21st Century COE program for “Towards a New Basic Science; Depth and Synthesis,” and the Grant-in-Aid for Scientific Research (No. 14204053) from the Japan Society for the Promotion of Science. We thank Drs. E. Ito and O. Ohtaka for help in synthesizing MgSiO₃- and MgGeO₃-ilmenite using multi-anvil apparatuses.

References

ASHIDA, T., KUME, S., ITO, E. AND NAVROTSKY, A., 1988. MgSiO₃ ilmenite: heat capacity, thermal expansivity, and enthalpy of transformation. *Phys. Chem. Miner.*, 16, 239-245.

ASHIDA, T., MIYAMOTO, Y. AND KUME, S., 1985. Heat capacity, compressibility and thermal expansion coefficient of ilmenite-type MgGeO₃. *Phys. Chem. Miner.*, 12, 129-131.

FATELEY, W.G., McDEVITT, N.T. AND BENTLY, F.F., 1971. Infrared and Raman selection rules for lattice vibrations: the correlation method. *Appl. Spectrosc.*, 25, 155-174.

GILLET, P., RICHET, P., GUYOT, F. AND FIQUET, G., 1991. High-temperature thermodynamic properties of forsterite. *J. Geophys. Res.*, 95, 21635-21655.

GILLET, P., Guyot, F. AND MALEZIEUX, J.M., 1989. High-pressure and high-temperature Raman spectroscopy of Ca₂GeO₄: some insights on anharmonicity. *Phys. Earth Planet. Int.*, 58, 141-154.

HOFMEISTER, A.N., 1993. IR reflectance spectra of natural ilmenite: comparison with isostructural compounds and calculation of thermodynamic properties. *Eur. J. Miner.*, 5, 281-295.

HOFMEISTER, A.N. AND ITO, E., 1992. Thermodynamic properties of MgSiO₃ ilmenite from vibrational spectra. *Phys. Chem. Miner.*, 18, 423-432.

HORIUCHI, H., HIRANO, M., ITO, E. AND MATSUI, Y., 1982. MgSiO₃ (ilmenite-type): single crystal X-ray diffraction study. *Am. Miner.*, 67, 788-793.

KARKI, B.B., DUAN, W., DA SILVA, C.R.S. AND WENTZCOVITCH, R.M., 2000. Ab initio structure of MgSiO₃ ilmenite at high pressure. *Am. Miner.*, 85, 317-320.

LIEBERMANN, R.C., 1976. Elasticity of ilmenites. *Phys. Earth Planet. Int.*, 12, 5-10.

LINTON, J.A., FEI, Y. AND NAVROTSKY, A., 1999. The MgTiO₃-FeTiO₃ join at high pressure and temperature. *Am. Miner.*, 84, 1595-1603.

MATSUI, M., AKAOGI, M. AND MATSUMOTO, T., 1987. Computational model of the structural and elastic properties of the ilmenite and perovskite phase of MgSiO₃. *Phys. Chem. Miner.*, 14, 101-106.

MAO, H.K., BELL, P.M., SHANER, J.W. AND STEINBERG, D.J., 1978. Specific volume measurements of Mo, Pd, and Ag and calibration of ruby R1 fluorescence pressure gauge from 0.06 to 1Mbar. *Jour. Appl. Phys.*, 49, 3276-3283.

McMILLAN, P.F. AND ROSS, N.L., 1987. Heat capacity calculations for Al₂O₃ corundum and MgSiO₃ ilmenite. *Phys. Chem. Miner.*, 16, 225-234.

POIRIER, J.P., 1991. *Introduction to the Physics of the Earth's Interior*. Cambridge: Cambridge University Press.

REYNARD, B., FIQUET, G., ITIE, J-P. AND RUBIE, D.C., 1996. High-pressure X-ray diffraction study and equation of MgSiO₃ ilmenite. *Am. Miner.*, 81, 45-50.

REYNARD, B. AND RUBIE, D.C., 1996. High-pressure, high-temperature Raman spectroscopic study of ilmenite-type MgSiO₃. *Am. Miner.*, 81, 1092-1096.

ROSS, N.L. AND McMILLAN, P., 1984. The Raman spectrum of MgSiO₃ ilmenite. *Am. Miner.*, 69, 719-721.

ROSS, N.L. AND NAVROTSKY, A., 1988. Study of the MgGeO₃ polymorphs(orthopyroxene, clinopyroxen and ilmenite structures) by calorimetry, spectroscopy and phase equilibria. *Am. Miner.*, 97, 1355-1365.

SAWAMOTO, H., 1987. Phase diagram of MgSiO₃ at pressure up to 24 GPa and temperatures up to 2200 C: phase stability and properties of tetragonal garnet. *In: M.H. MANGHNANI, Y. SYONO, eds. High-pressure in mineral physics*, Tokyo: Terrapub, 209-219

TOMIOKA, N. AND FUJINO, K., 1997. Natural (Mg, Fe)SiO₃-ilmenite and perovskite in the Tenham Meteorite. *Science*, 277, 352-355.

WECHSLER, B.A. AND PREWITT, C.T., 1984. Crystal structure of ilmenite (FeTiO₃) at high temperature and at high pressure. *Am. Miner.*, 69, 176-185.

WEIDNER, D.J. AND ITO, E., 1985. Elasticity of MgSiO₃ in the ilmenite phase. *Phys. Earth Planet. Int.*, 40, 65-70.

WHITE, W.B., 1974. Order-disorder effects. *In: V.C. FARMER, ed. The Infrared Spectra of Minerals*, London: Mineralogical Society, 87-91.

YAMANAKA, T., KOMATSU, Y., SUGAHARA, M. AND NAGAI, T., 2005. Structure change of MgSiO₃, MgGeO₃ and MgTiO₃ ilmenites under compression. *Am. Miner.*, in press.